J. Synchrotron Rad. (1998). **5**, 1149–1152

Design of beamline optics for EUVL

Takeo Watanabe,[a*] Tsuneyuki Haga,[b] Masahito Niibe[a] and Hiroo Kinoshita[a]

[a]Himeji Institute of Technology, 2167 Shosha, Himeji, Hyogo 671-22, Japan, and [b]NTT System Electronics Laboratories, 3-1 Morinosato Wakamiya, Atsugi, Kanagawa 243-01, Japan. E-mail: takeo@lasti.himeji-tech.ac.jp

(*Received 4 August 1997; accepted 21 November 1997*)

The design of front-end collimating optics for extreme-ultraviolet lithography (EUVL) is reported. For EUVL, collimating optics consisting of a concave toroidal mirror and a convex toroidal mirror can achieve shorter optical path lengths than collimating optics consisting of two concave toroidal mirrors. Collimating optics consisting of a concave toroidal mirror and a convex toroidal mirror are discussed. The design of collimating optics for EUVL beamlines based on ray-tracing studies is described.

Keywords: extreme-ultraviolet lithography (EUVL); collimating optics; beamline design; toroidal mirrors.

1. Introduction

With the goal of promoting industrial applications of synchrotron radiation, Hyogo Prefecture is constructing a synchrotron storage ring, New SUBARU, which will be operated at an energy of 1.5 GeV, on the SPring-8 site. In March 1998, electrons for this ring will be available from the injector of SPring-8 and commissioning will commence.

A beamline for EUVL (Kinoshita *et al.*, 1989, 1993; Jewell *et al.*, 1990; Haga & Kinoshita, 1995) will be installed at New SUBARU for an industrial applications program. We have chosen a bending-magnet beamline for EUVL. The ring parameters of New SUBARU for this beamline are shown in Table 1.

EUVL for semiconductor manufacturing requires collimating optics to satisfy throughput demands. The collimating optics project light from the bending-magnet source onto the mask with a large area. The mask pattern can be replicated onto a wafer through the imaging optics, which consist of multilayer-coated mirrors. EUVL employs multilayer-coated-mirror imaging optics at a wavelength of 13 nm (Kurihara *et al.*, 1991; Kinoshita *et al.*, 1993, 1997; Cook, 1981; Mashima, 1997; Watanabe *et al.*, 1997; Namioka *et al.*, 1995). The collimating optics are employed in the collection of X-rays from a very wide aperture and to provide an image, in combination with the imaging optics, that is matched to the requirements of the exposure system.

Ray-tracing studies using *SHADOW* (Lai *et al.*, 1988) were performed to design the specifications for the collimating optics and also to determine their optimum positions in the beamline. The design of the collimating optics for EUVL beamlines based on ray-tracing studies is described in this paper.

2. Design concepts for collimating optics for an EUVL beamline

In order to design collimating optics for an EUVL beamline, the three following parameters are important: (i) beam sizes at the exposure point have to be larger than ±20 mm in the horizontal direction and ±10 mm in the vertical direction, (ii) beam divergences at the last mirror before the mask have to be less than ±1 mrad in both the horizontal and vertical directions, and (iii) the distance between the source and the first toroidal mirror is 2.7 m and the distance between the source and the second mirror has to be less than 4.0 m.

We compared two possible cases employing two toroidal mirrors for the front-end mirror optics. Toroidal mirrors are less complicated to fabricate than ellipsoid and paraboloid mirrors and are much easier to fabricate than some of the more complex aspherical surfaces proposed. In case *A*, the collimating optics consist of a concave toroidal mirror as the first mirror (T1) and a convex toroidal mirror as the second mirror (T2) in the beamline. In case *B*, the collimating optics consist of two concave toroidal mirrors, T1 and T2.

Table 1
The ring parameters of New SUBARU storage ring.

Circumference	118.716 m
Electron energy	1.5 GeV
Beam current	500 mA
Bending radius	3.219 m
Horizontal emittance	67π nm rad
Vertical emittance	6.7π nm rad
Horizontal beam size	0.296 mm
Vertical beam size	0.317 mm
Horizontal divergence	±12 mrad
Vertical divergence	±1.9 mrad

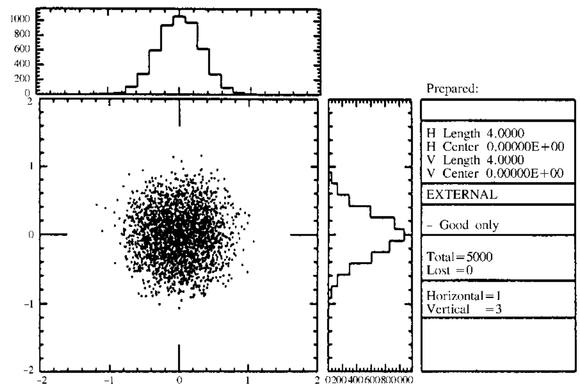

(*a*)

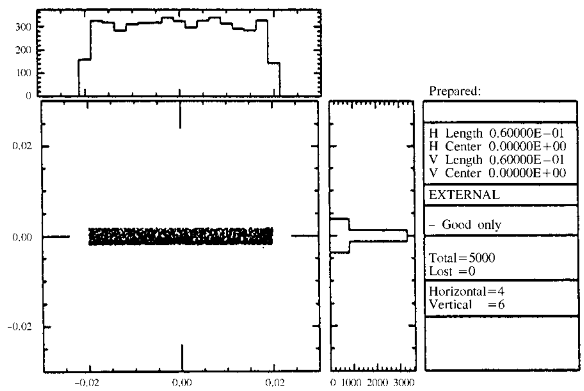

(*b*)

Figure 1
The bending-magnet source for EUVL beamlines, (*a*) the beam image and (*b*) the beam divergence. Tick-marks in (*a*) and (*b*) correspond to 1 mm and 0.02 rad, respectively.

Table 2
The designed parameters of mirrors for collimating optics, which consist of a concave toroidal T1 mirror and a convex toroidal T2 mirror.

First mirror (concave toroidal mirror)

Distance from source	2.7 m
Horizontal acceptance angle	±20 mrad
Sagittal radius	120 mm
Tangential radius	89.721 m
Mirror width	120 mm
Mirror length	450 mm

Second mirror (convex toroidal mirror)

Distance from first mirror	1.2 m
Sagittal radius	84 mm
Tangential radius	642.006 m
Mirror width	50 mm
Mirror length	350 mm

Figs. 1(a) and 1(b) show the beam spot and beam divergence, respectively, at the bending-magnet source at a wavelength of 13 nm for EUVL. In Fig. 1, the horizontal axis (X axis) corresponds to the horizontal direction and the vertical axis (Y axis) corresponds to the vertical direction. The horizontal divergence X' (dX/dZ) is about ten times greater than the vertical divergence Y' (dY/dZ). Collimation in the horizontal (XZ) plane is, therefore, more important than in the vertical (YZ) plane.

The optical paths for case A and case B in the XZ plane are shown in Figs. 2(a) and 2(b), respectively. The distance between the source point and the T2 mirror in case A is shorter than in case B.

3. Optimization of the collimating optics

The collimating optics consisting of a concave toroidal T1 mirror and a convex toroidal T2 mirror were then optimized. The distance between the source point and the T1 mirror is fixed at 2.7 m, which is the minimum length for the front-end component at New SUBARU, and the distance between the T1 and T2 mirrors is 1.2 m, which is the minimum length for installing the T1 and T2 mirror chambers. The optimum parameters for the focal length f_{1x} of the T1 mirror in the downstream direction of the XZ plane and the focal length f_{1y} ($= nf_{1x}$) of T1 in the downstream direction of the YZ plane, are shown in Fig. 3. Instead of varying the focal-length parameter f_{1y}, the parameter n in $f_{1y} = nf_{1x}$ was varied.

Focal lengths f_{1x} of 1.5, 2.0 and 3.0 m were considered in the optimization of n. Figs. 4, 5 and 6 show the relation between n and both the beam divergence and the number of rays lost down-

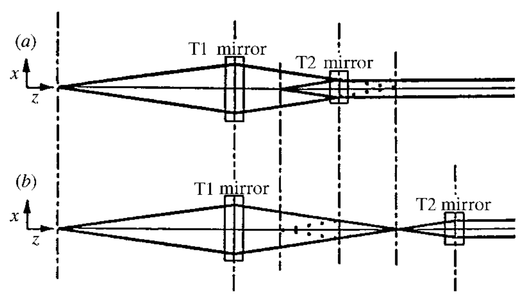

Figure 2
The comparison between (a) the collimating optics consisting of a concave toroidal T1 mirror and a convex toroidal T2 mirror and (b) the collimating optics consisting of two concave toroidal mirrors.

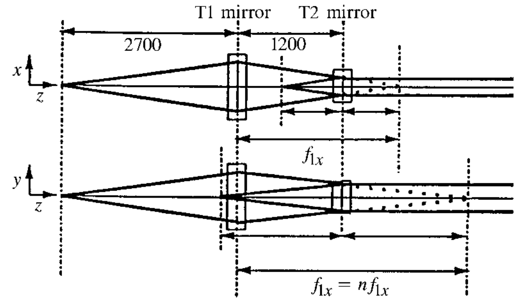

Figure 3
Parameters for the collimating optics consisting of a concave toroidal T1 mirror and a convex toroidal T2 mirror.

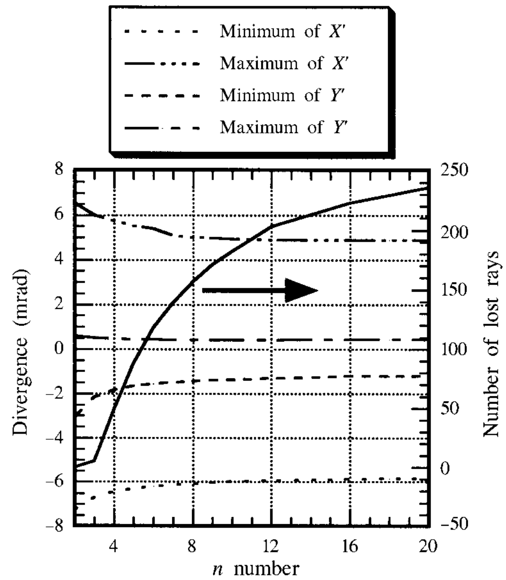

Figure 4
The relation between n and the beam divergence and number of rays lost downstream of the second mirror, for a first mirror T1 of focal length 1.5 m. X' ($= dX/dZ$) and Y' ($= dY/dZ$) indicate the horizontal and vertical beam divergences, respectively.

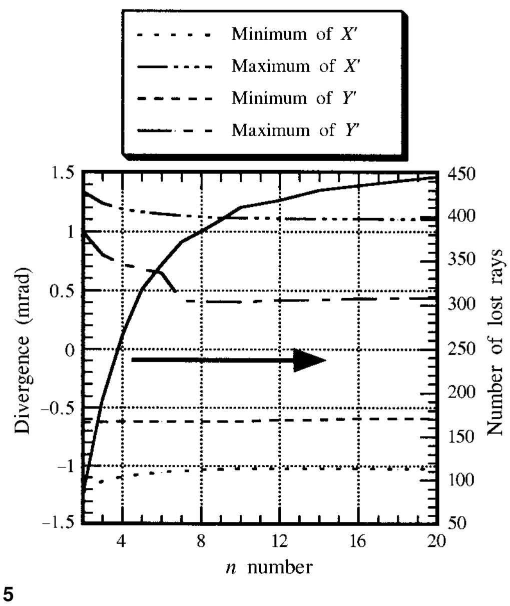

Figure 5
As Fig. 4, but for a T1 mirror of focal length 2.0 m.

stream for the T2 mirror when f_{1x} = 1.5, 2.0 and 3.0 m, respectively. For all three cases, beam divergence after the *T2* mirror is minimal and practically independent of n when $n > 9$, although the number of rays lost increases with increasing values of n values. Thus the n value is optimized at $n = 9$.

Fig. 7 shows the dependence of the beam divergence after T2 and the numbers of rays lost when $n = 9$. The beam divergence varies only slightly for $f_{1x} > 2.0$ m, and both a horizontal beam divergence X' and a vertical beam divergence Y' of less than ± 1 mrad can be achieved. As the focal length f_{1x} increases, the number of lost rays also increases. Thus the optimum focal length f_{1x} is approximately 2000 mm.

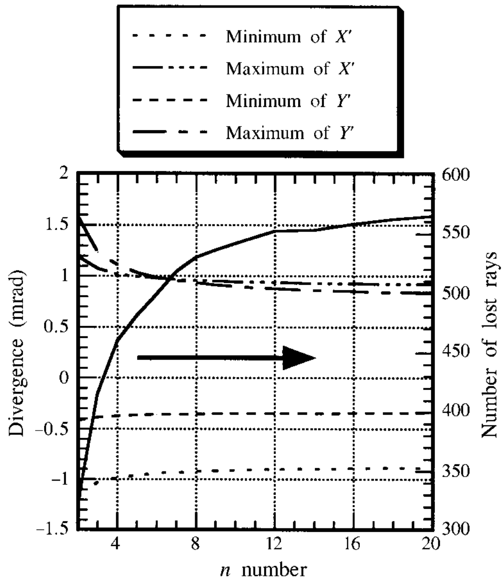

Figure 6
As Fig. 4, but for a T1 mirror of focal length 3.0 m.

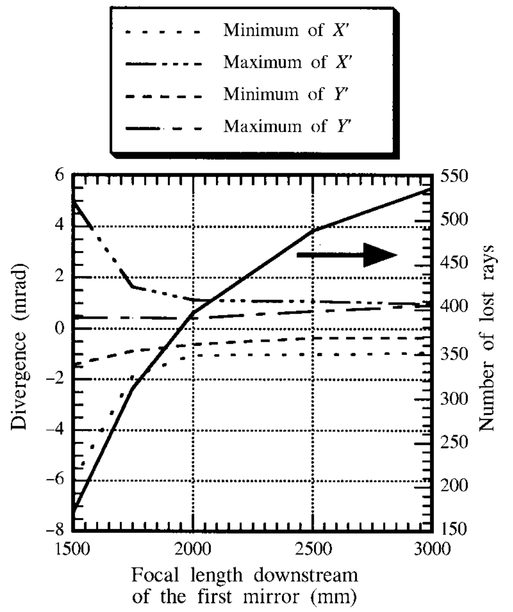

Figure 7
The dependence of beam divergence and number of rays lost downstream of the second mirror T2 when $n = 9$. X' (= dX/dZ) and Y' (= dY/dZ) indicate horizontal and vertical beam divergence, respectively.

For $n = 9$ and $f_{1x} = 2.0$ m, the optimized design parameters for the T1 and T2 mirrors are shown in Table 2. A cross section of the beam spot and the divergence at a distance of 18 m from the T2 mirror are shown in Figs. 8(*a*) and 8(*b*), respectively. In Fig. 8, the horizontal axis corresponds to the horizontal direction and the vertical axis corresponds to the vertical direction. Tick-marks in Figs. 8(*a*) and 8(*b*) correspond to 50 mm and 2 mrad, respectively. At a point 18000 mm downstream of the second mirror, the beam size is about ± 20 mm in the horizontal direction and about ± 10 mm in the vertical direction, and the beam divergence is ± 1 mrad in the horizontal direction and ± 0.5 mrad in the vertical direction. The beam image and the beam divergence at 18 m satisfy the specification for the collimating optics. Furthermore, as the distance between the second mirror T2 and the source is 3.9 m, the original specification that this distance should be shorter than 4.0 m is also satisfied. An exposure field 40 $\times$ 10 mm in size with a homogeneity of within 2% at the mask is achieved.

4. Conclusions

A collimating optical system consisting of a concave toroidal mirror and a convex toroidal mirror has a shorter optical path length than a system with two concave toroidal mirrors. Ray-tracing calculations were used to optimize the focal lengths, divergence and throughput. The requirements for the collimating optics for an EUVL beamline were achieved at 18 m from the convex toroidal mirror.

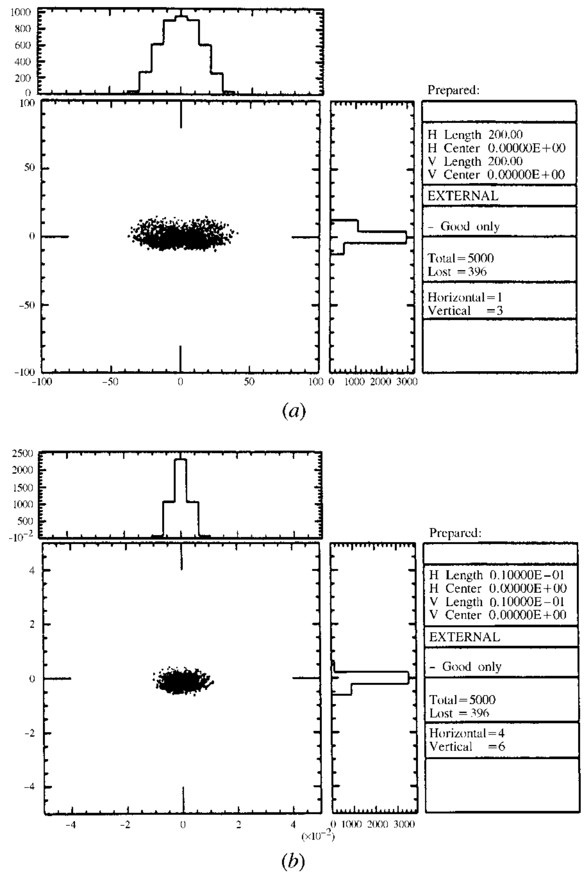

Figure 8
(*a*) Beam image at a distance of 18 m from the second mirror T2 and (*b*) the divergence in horizontal and vertical planes. Tick-marks in (*a*) and (*b*) correspond to 50 mm and 2 mrad, respectively.

References

Cook, L. G. (1981). US Patent 4 265 510.

Haga, T. & Kinoshita, H. (1995). *J. Vac. Sci. Technol. B*, **13**(6), 2914–2918.

Jewell, T. E., Rodgers, J. M. & Thompson, K. P. (1990). *J. Vac. Sci. Technol. B*, **8**, 1519–1523.

Kinoshita, H., Kurihara, K., Ishii, Y. & Torii, Y. (1989). *J. Vac. Sci. Technol. B*, **7**, 1648–1651.

Kinoshita, H., Kurihara, K., Mizota, T., Haga, T., Takenaka, H. & Torii, Y. (1993). *Appl. Opt.* **32**, 7079–7083.

Kinoshita, H., Watanabe, T., Koike, M. & Namioka, T. (1997). *Proc. SPIE*, **3152**, 211–220.

Kurihara, K., Kinoshita, H., Takeuchi, N., Mizota, T., Haga, T. & Torii, Y. (1991). *J. Vac. Sci. Technol. B*, **9**, 3189–3192.

Lai, B., Chapman, K. & Cerrina, F. (1988). *Nucl. Instrum. Methods A*, **266**, 544–549.

Mashima, K. (1997). *JSPE Proceedings of the Second US–Japan Workshop on Soft X-ray Optics*, pp. 306–315. Tokyo: The Japan Society for Precision Engineering.

Namioka, T., Koike, M., Kinoshita, H. & Haga, T. (1995). *Proc. SPIE*, **2576**, 94–104.

Watanabe, T., Kinoshita, H. & Niibe, M. (1997). *JSPE Proceedings of the Second US–Japan Workshop on Soft X-ray Optics*, pp. 341–348. Tokyo: The Japan Society for Precision Engineering.